Preprint Title Preparation of a sunlight-driven TiO_2 film with excellent material characterizations and photoelectrocatalytic properties by an eco-friendly manner

Authors Chang-Xin Li, Yan Liu, Yan-Zong Zhang, Lu-Lu Long, Fei Shen, Gang Yang, Xiao-Hong Zhang, Yan He, Li-Lin Wang and Shi-Huai Deng

Article Type Full Research Paper

ORCID® iDs Yan-Zong Zhang - https://orcid.org/0000-0002-4222-0445

Preparation of a sunlight-driven TiO_2 film with excellent material characterizations and photoelectrocatalytic properties by an eco-friendly manner

Chang-Xin Li[1], Yan Liu[1], Yan-Zong Zhang*[1], Lu-Lu Long[1,2], Fei Shen[1,2], Gang Yang[1,2], Xiao-Hong Zhang[1], Yan He[1], Li-Lin Wang[1] and Shi-Huai Deng[1,2]

Address: [1] College of Environment, Sichuan Agricultural University, Chengdu, Sichuan 611130, China and [2] Institute of Ecological and Environmental Sciences, Sichuan Agricultural University, Chengdu, Sichuan 611130, China

Email: Yan-Zong Zhang* - yzzhang@sicau.edu.cn.

* Corresponding author

Abstract

A hybrid structure of $(NO_x)_i/S^{6+}$-TiO_2 (x=0,1) film with high visible-light activity was prepared via facile one-step anodizing in $(NH_4)_2S_2O_8$ electrolyte. The film was characterized by scanning electron microscopy, X-ray photoelectron spectroscopy, X-ray diffraction, and ultraviolet-visible-infrared absorption spectroscopy, respectively. Transient photocurrent response and linear sweep voltammetry were also detected. The results showed that the $(NO_x)_i/S^{6+}$-TiO_2 film was composed of “flower-like” and porous structure. And N and S were successfully doped in the film. Meanwhile, the

film also displayed broad and strong optical absorption at around 544 nm and 1500 nm. The photocurrent density reached 0.71 mA/cm^2. The decoloration rate was close to 100% and TOC removal reached 59.44% in 20 min under sunlight in photoelectrocatalytic (PEC) degradation methyl orange. The film also exhibited good stability after reuse ten times. A possible mechanism of PEC was suggested in methyl orange degradation by using $(NO_x)_i/S^{6+}$-TiO_2 film.

Keywords

Anodizing; N/S co-doping; Narrow-gap; Photoelectrocatalytic; Mechanism

Introduction

TiO_2 films have been widespread employed as the photocatalyst owing to its non-toxicity, chemical stability and less secondary pollution [1-3]. However, low utilization rate of sunlight due to wide band gap (3.2 eV for anatase), low specific surface area and low separation efficiency of electron-hole pairs obviously decreases its photocatalytic activities [4, 5]. Therefore, many efforts have carried out to overcome these limitations.

The nonmetal (especially N, S) doping can efficiently narrow the band gap of TiO_2 films and enhance absorption of visible light [6-9]. Therefore, N and S doping is recognized as one of the most promising research. Such as N-doped TiO_2 narrow the bandgap through forming NO bond with the π character at interstitial lattice sites [10]. So far, to ensure N- or S-dopants into the TiO_2 film lattices, almost all N- and S-TiO_2 films are prepared in NH_3 or H_2S atmosphere at high temperature [11]. These methods not only cause energy waste, but also have harsh preparation conditions. The

problems can be avoided by the anodizing methods [12], while anodizing electrolytes are complex and environmentally unfriendly [13-17]. Therefore, eco-friendly electrolytes have been become the key to solve the problem. Persulfate (PS, $S_2O_8^{2-}$), a strong oxidant, could be activated to produce stronger sulfate radical ($SO_4^{\bullet-}$) by electron transfer, heat, ultrasound and other methods [18-21] (Eq. 1). Sulfate radicals can obtain electrons from ammonia nitrogen (NH^{4+} and NH_3) in pH value of 3-8.3, and oxidize them to N_2 and NO_x (Eq. 2) [19]. PS is reduced to inert sulfate anions as final product that not be considered as pollutants.

$$S_2O_8^{2-}+e^-/\text{ energy /heat} \rightarrow SO_4^{\cdot-}+SO_4^{2-} \quad (1)$$

$$SO_4^{\cdot-}+NH_4^+/\ NH_3 \rightarrow N_2\uparrow+NO_X(\text{molecules})+SO_4^{2-} \quad (2)$$

In order to simultaneously introduce N- and S- into TiO_2 lattices, ammonium persulfate ($(NH_4)_2S_2O_8$) was used for oxidant and electrolyte to fabricate a $(NO_x)_i/S^{6+}$-TiO_2 films via anodizing in this study. The morphology, crystal structure, chemical composition, optical properties, and photoelectrochemical activities were investigated. The photoelectrocatalytic (PEC) activity of $(NO_x)_i/S^{6+}$-TiO_2 film was confirmed by methyl orange as a target pollutant.

Results and Discussion

Morphology analysis

Many local defects were distributed on the surface of Ti substrate after mechanical and chemical polishing (Fig. 1a). Some “flower-like” structures were formed on the surface of $(NO_x)_i/S^{6+}$-TiO_2 film (Fig. 1b and 1c), and a large number of microvoids were distributed around them (Fig. 1b and 1d). The rough Ti substrate caused

non-uniform electric field, especially at these local defects at high anodizing voltage [22]. The defects acted as crystal nucleation sites, and the nitric and thionic ions focused preferentially on these sites (Eq. 1 and 2). Therefore, the defects were easier etched, and further facilitated crystallization [23, 24], resulting in the formation of "flower-like" structures with the increase of anodizing time. Meanwhile, many microvoids with different depth were also formed in the direction of different electric intensity (Fig. 1d) [22].

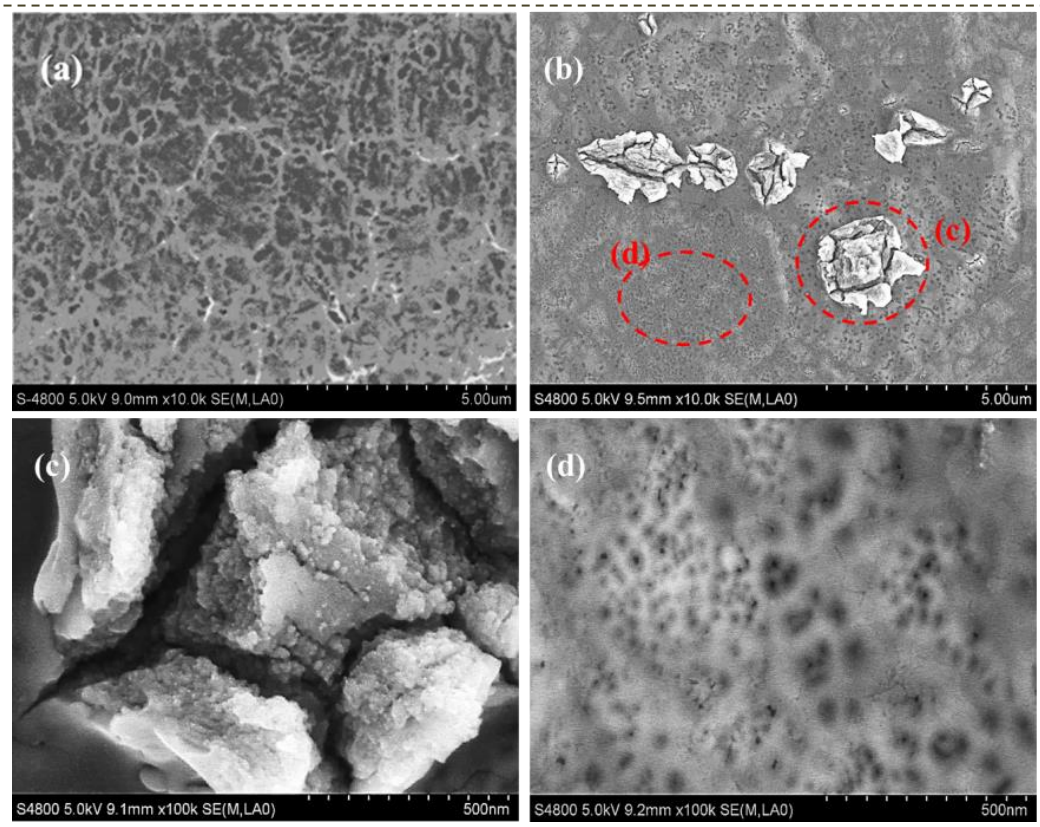

Fig. 1 FE-SEM images of (a) Ti substrate, (b) $(NO_x)_i/S^{6+}$-TiO_2 film, (c) and (d) Local enlarged images in (b).

Elemental composition and crystal structure analysis

C, S, N, O and Ti were detected on the surface of $(NO_x)_i/S^{6+}$-TiO_2 film (Fig. 2a). The C element was derived from adventitious carbon-based contaminant in XPS instrument.

Only one weak peak of S 2p (0.28 at%) located at 168.88 eV (inset of Fig. 2a), indicating that less S^{6+} state were interstitially incorporated into the TiO_2 lattice [25]. The peak at 399.22 eV was ascribed to interstitial N in Ti-O-N bond [26, 27] (Fig. 2b), and the peak at 401.14 eV usually attributed to NO[28, 29]. It was possible that the NO molecules produced by Eq. 2 or oxidation reaction of residual NH_4^+ at high temperature on the film surface, which were trapped in the microvoids or incorporated with TiO_2 lattice [30, 31]. Ti^{4+}-O bonds were confirmed from the Ti $2p_{3/2}$ (459.82 eV) and Ti $2p_{1/2}$ (465.52eV) peaks (Fig. 2c) [32]. Two high binding energy peaks of O 1s at 531.09 and 532.94 eV were attributed to the OH groups on the film surface and oxygen of NO_x/oxysulfide, respectively (Fig. 2d) [6, 33]. The existence of OH groups could promote its hydrophilicity, and was conducive to the PEC degradation of organic pollutants [34, 35]. The atomic ratio of O and Ti was 2.41. It meant that there was titanium oxynitride (oxysulfide) in the $(NO_x)_i/S^{6+}$-TiO_2 film. Binding energy of elements shifted to high energy, indicating that electrons were easier to flow to N and S dopants that combined with titanium oxide, thus reducing the recombination of e^-/h^+ pairs [10].

The Ti substrate displayed only titanium crystal peaks (Fig. 3a), while two diffraction peaks of anatase phase appeared in the $(NO_x)_i/S^{6+}$-TiO_2 film at 25.26° (101) (PDF#:21-1272) and 48.02° (Fig. 2b). The width and intensity of the (101) peak was broad and strong, indicating the smaller crystallite size and higher crystallinity[36]. The crystallite size was calculated from the XRD patterns by Scherrer's equation (Table 1). It was confirmed that N and S co-doping could efficiently inhibit crystallite growth [37]. Furthermore, N and S co-doping effectively promoted the formation of anatase TiO_2,

thereby increasing the film's photoresponsive activity [38].

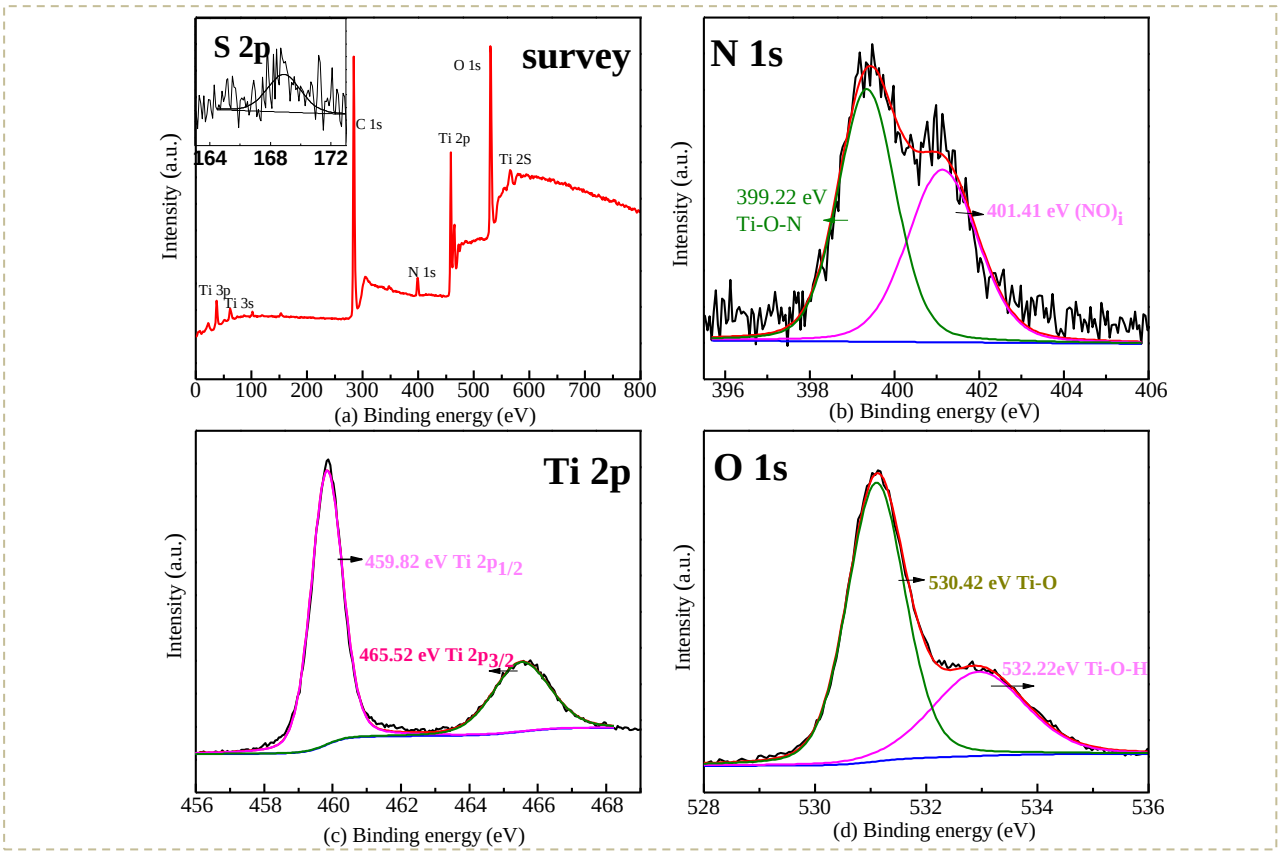

Fig. 2 XPS spectra of $(NO_x)_i/S^{6+}$-TiO_2 film. (a) Full survey spectrum and the inset was S 2p, (b) N 1s, (c) Ti 2p and (d) O 1s.

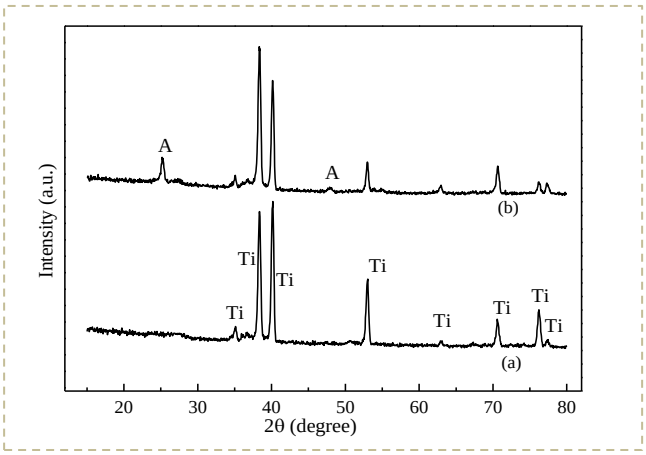

Fig. 3 XRD patterns of the simples. (a) Ti substrate, (b) $(NO_x)_i/S^{6+}$-TiO_2 film**.**

Table 1 The crystal size of $(NO_x)_i/S^{6+}$-TiO_2 film

Catalysts ID		d (Å)	FWHM	Crystal size (nm)
Ti substrate	*	-	-	-
$(NO_x)_i/S^{6+}$-TiO_2	A	3.5274	0.447	18.7

"-": No data, "*": titanium crystal, "A": Anatas.

Optical properties analysis

Almost no absorption peak was found for Ti substrate (Fig. 4a). However, major absorption peaks appeared in visible region (544 nm) and near infrared region (around 1500 nm) for the $(NO_x)_i/S^{6+}$-TiO_2 film. To determine the band gap energies, a plot of $(Ahv)^2$ vs hv was shown in Fig. 4b. The $(NO_x)_i/S^{6+}$-TiO_2 film displayed lower band gap energy (1.78 and 0.45 eV). The band gap at 1.78 eV was ascribed to the formation of delocalized state above the valence band (VB) because of interstitial N/S 2p and O 2p interaction [31]. The band gap at 0.45 eV may be caused by the NO bond with π character generating new localized states between the valence band and conduction band (CB) [39]. Therefore, broad optical absorption and the narrow bandgap indicating that N, S co-doping were beneficial to improve the utilization of solar energy.

Measurement of photoelectrochemical activity

The photocurrent response of $(NOx)_i/S^{6+}$-TiO_2 film was investigated to evaluate photocatalytic performances under sunlight (Fig. 5a). It showed a high photocurrent density of 0.71 mA/cm^2, and exhibited good stability and reproducibility. This result suggested that electrons could rapidly transport from VB to CB. The photocurrent density obviously increased with the increase of bias voltage (Fig. 5b), indicating that

the applied potential could facilitate the separation of the e^-/h^+ pairs, and thereby improved the PEC activity.

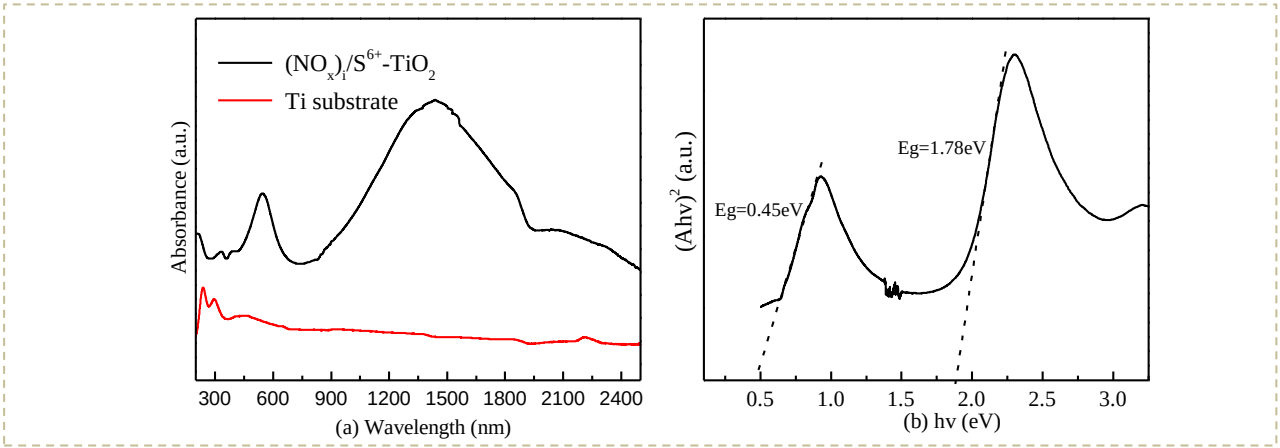

Fig. 4 (a) UV-vis absorption spectra of Ti substrate and $(NO_x)_i/S^{6+}$-TiO_2 film, (b) Plots of transformed Kubelka-Munk for band gap energy in UV–vis absorption spectra.

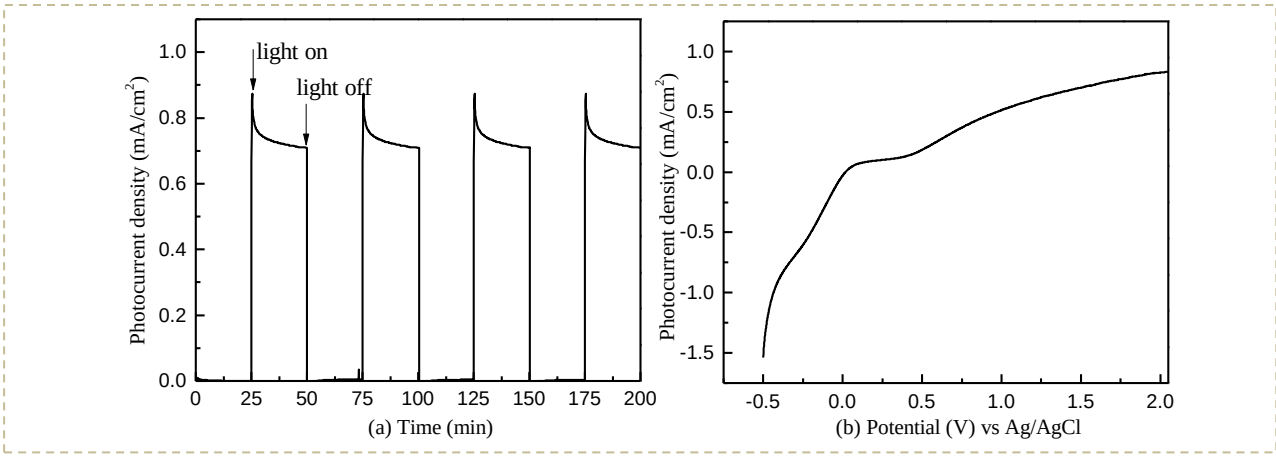

Fig. 5 (a) Photocurrent response of $(NO_x)_i/S^{6+}$-TiO_2 film under sunlight with a potential bias of 0 V vsAg/AgCl, (b) photocurrent density−voltage curves of $(NO_x)_i/S^{6+}$-TiO_2 film in voltage range of -1.0 to 2.0 V vs Ag/AgCl.

Evaluation of photoelectrocatalytic activity

The direct photolysis efficiency of MO was only 6.56% under sunlight (Fig. 6a). However, the MO decoloration could reach almost 100% in 20 min in PEC process. Meanwhile, the absorption peak of MO at 466 nm diminished with increasing decoloration time (Fig. 6b). It indicated that MO almost completely decomposed into small and simple molecules [40]. Nevertheless, the TOC removal reached 59.44% after

20 min (Fig. 6c). It showed that the cleavage of chromophores mainly occurred at the initial stage, but the mineralization of the generated organic intermediates required longer time. In addition, the decoloration rate had no significant reduction after ten cycles (Fig. 6d). Degradation of other pollutants in this work was also listed in Table 2. The higher PEC activity of the $(NO_x)_i/S^{6+}$-TiO_2 film can be due to three key aspects. First, the hybrid structures could increase the specific surface area, and provide more active sites. Second, the introduction of $(NO_x)_i/S^{6+}$ narrowed the band gap significantly, heightening the quantum yield of sunlight. Third, suitable bias voltage accelerated the charge transfer, decreasing the recombination of e^-/h^+ pairs.

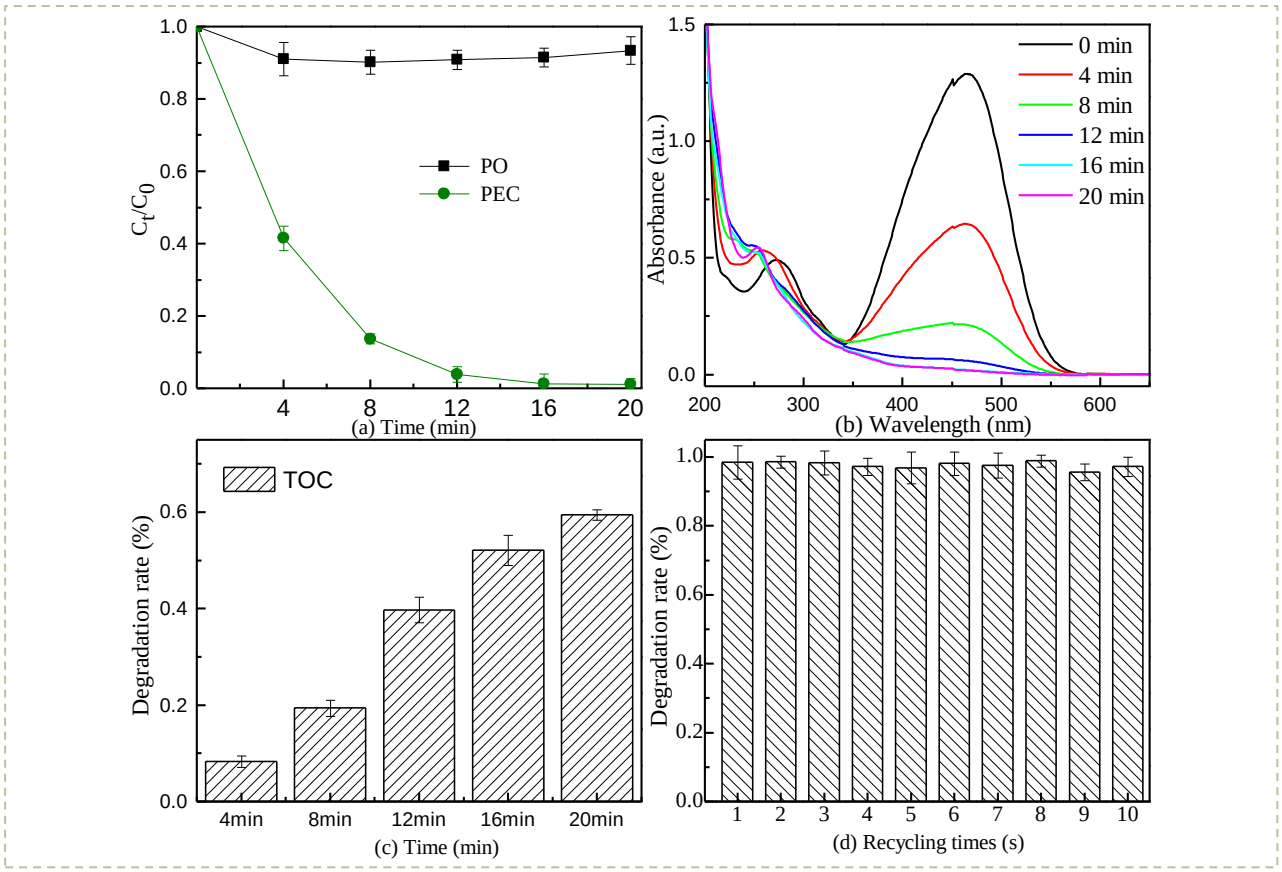

Fig. 6 (a) The MO decolorization rate under the conditions of PO (sunlight irradiation without photoelectrode and a 2.0 V bias), and PEC (photoelectrode under sun light irradiation with 2.0 V bias), (b) UV-vis scanning spectrum of MO solution during PEC process of $(NO_x)_i/S^{6+}$-TiO_2 film, (c) TOC removal under sunlight, (d) recycling tests of PEC decoloration under sunlight (reaction conditions: 2.0 V, 0.05M NaCl, pH =

6.5±0.2, 20 mg/L MO, 50 mL solution).

Table 2 Degradation of different simulated pollutants using $(NO_x)_i/S^{6+}$-TiO_2 film with the same reaction conditions.

Simulated pollutants	c_o (mg/ L)	Reaction conditions	Self-degradation %	Degradation rate %
Methylene blue	20	50 mL of solution with 0.1 M NaCl, 500 W Xe (AM 1.5g) for 20min, 25 ℃	8.77	98.13
Nitrobenzene	20	50 mL of solution with 0.1 M NaCl, 500 W Xe (AM 1.5g) for 120 min, 25 ℃	40.15	90.63

Degradation mechanism for PEC

The generation of active species, such as $\cdot O_2^-$, ·OH and h^+ could be expressed by Eq. (5), (6), (7), (8), (9), (10) and (11) in the PEC reaction [35].

$$TiO_2 \text{ film} + \text{sunlight} \rightarrow h^+_{VB} + e^-_{CB} \quad (5)$$

$$h^+_{VB} + H_2O \rightarrow H^+ + \cdot OH \quad (6)$$

$$e^-_{CB} + O_2 \rightarrow \cdot O_2^- \quad (7)$$

$$e^-_{CB} + O_2 + H^+ \rightarrow H_2O_2 \quad (8)$$

$$e^-_{CB} + H_2O_2 \rightarrow \cdot OH + OH^- \quad (9)$$

$$\cdot O_2^- + H_2O_2 \rightarrow \cdot OH + OH^- \quad (10)$$

$$h^+_{VB} + OH^- \rightarrow \cdot OH \quad (11)$$

The effect of different radicals was verified by adding radical scavengers into the reaction system (Fig. 7a). The EDTA-2Na (h^+ scavengers) and PBQ ($\cdot O_2^-$ scavengers) significantly inhabited the MO degradation while TB (·OH scavengers) hardly affected, that was, h^+ and $\cdot O_2^-$ radicals played important roles in the reaction process. In addition, to further determined the effect of hydroxyl radicals, we increased the

concentration of TB then found that MO degradation rate decreased obviously (Fig. 7b). This suggested that large amounts of hydroxyl were also produced in the process. Based on the above experimental and analysis results, a possible mechanism was proposed in Fig. 8. Interstitial N 2p and S 2p mixed with O 2p composed the VB. The interstitial NO with π character formed localized states between VB and CB. The electrons were excited and fast migrated from the VB to CB under sunlight irradiation. The active species including h^+ (Eqs. 5), h^+-created ·OH (Eqs. 6 and 11), hydroperoxide radicals (HR)-created ·OH (Eqs. 8, 9 and 10) and $\cdot O_2^-$ (Eqs. 7 and Ti cathode) were obtained and oxidized the adsorbed MO on the porous surface [41]. The electrons were easier to transfer from the film surface to Ti cathode when a suitable voltage was applied to the poles, resulting in higher separation efficiency of e^-/h^+ pairs. Hence, the degradation of MO was mainly attributed to the synergistic effect of h^+, $\cdot O_2^-$ and ·OH in the PEC process.

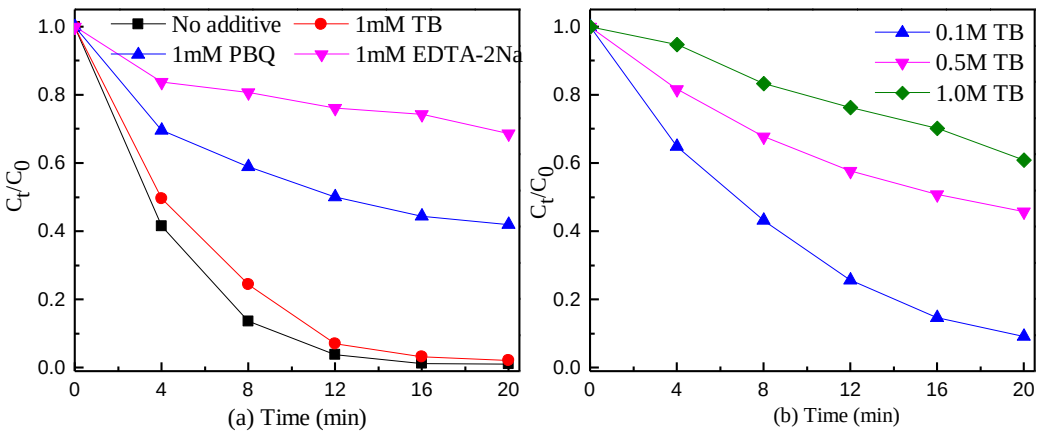

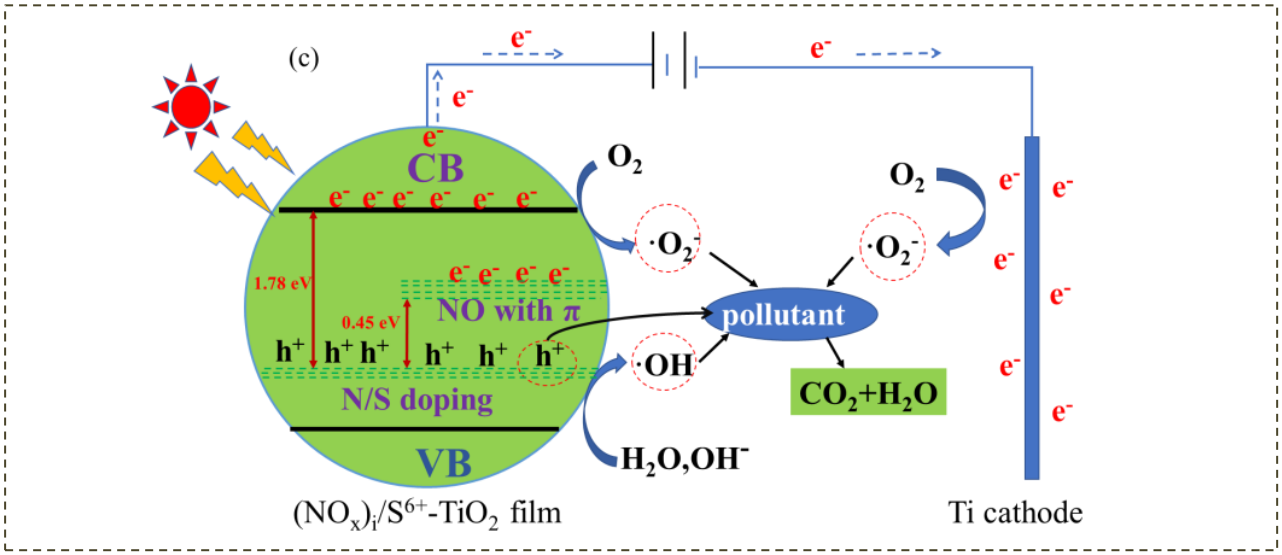

Fig. 7 Quenching of active species, (a) adding various scavengers, (b) adding different concentration of TB, (c) possible mechanism of PEC in the MO degradation by using $(NO_x)_i/S^{6+}$-TiO_2 film. (reaction conditions: 2.0 V, 0.05M NaCl, pH = 6.5±0.2, 20 mg/L MO, 50 mL solution).

Conclusions

In this study, we fabricated a N/S co-doping TiO_2 porous film on titanium foil using persulfate as eco-friendly electrolyte. The $(NO_x)_i/S^{6+}$-TiO_2 film has strong light absorption (from 290-2500 nm) and narrow-gap, which inhabit efficiently the recombination of electrons-holes. The film also exhibited high photoelectrochemical and PEC activity and stability under sunlight. On the whole, the film could be developed as a promising PEC material for practical application. It's also potential to be used as solar photovoltaic and near-infrared fluorescent materials due to highly efficient solar energy utilization.

Experimental

Materials

All chemicals (AR grade) were purchased from the Sinopharm Chemical Reagent Co., Ltd. China. Ti foil (purity 99.6%) was purchased from Baoji Jinbu Titanium Equipment Corporation, China. Ultrapure water (resistivity 18.2 MΩ·cm) was used in all

experiments.

Preparation of $(NO_x)_i/S^{6+}$-TiO_2 film

Ti foil was cut to 55 mm × 50 mm, and polished by 300 mesh sandpapers, then degreased in acetone, ethanol and ultrapure water for 15 min by ultra-sonication, respectively. Subsequently, these foils were polished in mixed solution of HF, HNO_3 and H_2O (volume ratio 1: 4: 5) until no bubbles, and rinsed in ultrapure water then dried at room temperature. The Ti foil was used as anode and Pt sheet was used as the cathode. The electrode separation kept 20 mm. The Ti foil was anodized for 5 min at 40 V in 0.01 M $(NH4)_2S_2O_8$ aqueous solution (80 mL, pH 4.34). All anodization steps were carried out at 35℃ in ultrasonic bath. After repeated rinsing in ultrapure water, the anodized samples were calcined at 773 K for 1h in muffle furnace, and then were taken out and cooled to ambient temperature. The simples were denoted as Ti substrate and $(NO_x)_i/S^{6+}$-TiO_2 film before and after anodizing, respectively.

Characterization of $(NO_x)_i/S^{6+}$-TiO_2 film

The morphology was observed by field-emission scanning electron microscopy (FE-SEM, S-4800, Hitachi). X-ray diffraction (XRD) analysis was performed on a X'Pert PRO diffractometer. X-ray photoelectron spectroscopy (XPS) measurements were conducted by Thermo Scientific Escalab 250 Xi XPS system. The UV-Vis-NIR absorption spectra were obtained using UV-3600 spectrometer in the range of 200-2500 nm with $BaSO_4$ reference. The photoelectrochemical measurements were carried out in 1 M Na_2SO_4 aqueous solution in three-electrode cell using electrochemical workstation (CHI 830C Instruments). The $(NO_x)_i/S^{6+}$-TiO_2 film and Pt foil were used as the working and counter electrode, respectively.

Photoelectrocatalytic experiments

The photoelectrocatalytic activity was carried out in a quartz photoreactor containing 50 ml MO solution (20 $mg \cdot L^{-1}$) with 0.05 M NaCl used as supporting electrolyte. The $(NO_x)_i/S^{6+}$-TiO_2 film acted as the photoanode, and the same size Ti foil acted as the photocathode (electrode spacing 5 mm). Bias potential of 2.0 V was applied to the

photoanode. The experiments were performed under 500 W Xenon lamp with an AM1.5G filter (GLORIA-X500A, Zolixin Struments Corporation, China). The irradiance was 850 $W \cdot m^{-2}$ at the distance of 100 mm. The average irradiation intensity was recorded by digital UV-C meter (ZDZ-1) and solar power meter (TES-1333). The absorbance of Methyl Orange (MO) solution was measured at 466 nm using UV-Vis spectrophotometer (UV 3000, China). The decolorization efficiency (D) was calculated as follows:

$$D = (C_0 - C_t) / C_0 \times 100\%. \quad (3)$$

Where C_0 ($mg \cdot L^{-1}$) was the initial concentration of MO, and C_t ($mg \cdot L^{-1}$) was the instantaneous concentration at a time (t).

TOC was measured by TOC analyzer (TOC-V CPH, Shimadzu). And the TOC removal (TOC_r) was calculated as following equation:

$$TOC_r = (TOC_0 - TOC_t)/TOC_0 \times 100\% \quad (4)$$

Where TOC_0 ($mg \cdot L^{-1}$) was the initial concentrations of MO, and TOC_t ($mg \cdot L^{-1}$) was remaining concentrations after the reaction.

Quenching experiments of active species

EDTA-2Na, p-benzoquinone (PBQ) and tertiary butanol (TB) were added in the MO solution as scavengers for holes (h^+), superoxide radicals ($\cdot O_2^-$) and hydroxyl radicals ($\cdot OH$), respectively [42, 43]. The testing procedure was similar to the above photoelectrocatalytic experiments.

Acknowledgments

This work was supported by the Science and Technology Department of Sichuan Province (2017JZ0021, 2017SZ0039) and the Education Department of Sichuan Province (17ZA0298).

References

1. Liu, C.; Ding, Y.; Wu, W.; Teng, Y. A simple and effective strategy to fast remove chromium (VI) and organic pollutant in photoelectrocatalytic process at low voltage, *Chemical Engineering Journal*, **2016**, *306*, 22-30.

2. Wang, Q.; Zhu, N.; Liu, E.; Zhang, C.; Crittenden, J. C.; Zhang, Y.; Cong, Y. Fabrication of visible-light active Fe_2O_3-GQDs/NF-TiO_2 composite film with highly enhanced photoelectrocatalytic performance, *Applied Catalysis B: Environmental*, **2017**, *205*, 347-356.

3. Gong, J.; Pu, W.; Yang, C.; Zhang, J. Tungsten and nitrogen co-doped TiO_2 electrode sensitized with Fe-chlorophyllin for visible light photoelectrocatalysis, *Chemical Engineering Journal*, **2012**, *209*, 94-101.

4. Zhou, X.; Zheng, Y.; Zhou, J.; Zhou, S. Degradation kinetics of photoelectrocatalysis on landfill leachate using codoped TiO_2/Ti photoelectrodes, *Journal of Nanomaterials*, **2015**, *2015*, 7.

5. Kmentová, H.; Nandan, D.; Kment, Š.; Naldoni, A.; Gawande, M. B.; Hubička, Z.; Zbořil, R. Significant enhancement of photoactivity in one-dimensional TiO_2 nanorods modified by S-, N-, O-doped carbon nanosheets, Catalysis Today, 2019, 328, 111-117.

6. Brindha, A.; Sivakumar, T. Visible active N, S co-doped TiO_2/graphene photocatalysts for the degradation of hazardous dyes, *Journal of Photochemistry and Photobiology A: Chemistry*, **2017**, *340*, 146-156.

7. Singh, P.; Vishnu, M. C.; Sharma, K. K.; Borthakur, A.; Srivastava, P.; Pal, D. B.; Tiwary, D.; Mishra, P. K. Photocatalytic degradation of Acid Red dye stuff in the

presence of activated carbon-TiO_2 composite and its kinetic enumeration, *Journal of Water Process Engineering*, **2016**, *12*, 20-31.

8. Gomathi Devi, L.; Kavitha, R. Review on modified N-TiO_2 for green energy applications under UV/visible light: selected results and reaction mechanisms, *RSC Adv.*, **2014**, *4*, 28265-28299.

9. Rahimi, N.; Pax, R. A.; Gray, E. M. Review of functional titanium oxides. I: TiO_2 and its modifications, *Progress in Solid State Chemistry*, **2016**, *44*, 86-105.

10.Di Valentin, C.; Finazzi, E.; Pacchioni, G.; Selloni, A.; Livraghi, S.; Paganini, M. C.; Giamello, E. N-doped TiO_2: Theory and experiment, *Chemical Physics*, **2007**, *339*, 44-56.

11.Asahi, R.; Morikawa, T. Nitrogen complex species and its chemical nature in TiO_2 for visible-light sensitized photocatalysis, *Chemical Physics*, **2007**, *339*, 57-63.

12.Momeni, M. M.; Ghayeb, Y.; Ghonchegi, Z. Visible light activity of sulfur-doped TiO_2 nanostructure photoelectrodes prepared by single-step electrochemical anodizing process, *Journal of Solid State Electrochemistry*, **2015**, *19*, 1359-1366.

13.Liu, Y.; Zhang, Y.; Wang, L.; Yang, G.; Shen, F.; Deng, S.; Zhang, X.; He, Y.; Hu, Y.; Chen, X. Fast and Large-Scale Anodizing Synthesis of Pine-Cone TiO_2 for Solar-Driven Photocatalysis, *Catalysts*, **2017**, *7*, 229.

14.Guisheng, L.; Ling, W.; Fang, L.; Pengpeng, X.; Dieqing, Z.; Hexing, L. Photoelectrocatalytic degradation of organic pollutants via a CdS quantum dots enhanced TiO_2 nanotube array electrode under visible light irradiation, *Nanoscale*, **2013**, *5*, 2118-2125.

15.Tan, B.; Zhang, Y.; Long, M. Large-scale preparation of nanoporous TiO_2 film on titanium substrate with improved photoelectrochemical performance, *Nanoscale Research Letters*, **2014**, *9*, 190.

16.Liu, Y.; Mu, K.; Zhang, Y.; Wang, L.; Yang, G.; Shen, F.; Deng, S.; Zhang, X.; Zhang, S. Facile synthesis of a narrow-gap titanium dioxide anatase/rutile nanofiber film on titanium foil with high photocatalytic activity under sunlight, *International Journal of Hydrogen Energy*, **2016**, *41*, 10327-10334.

17.Ansari, S. A.; Khan, M. M.; Ansari, M. O.; Cho, M. H. Nitrogen-doped titanium dioxide (N-doped TiO_2) for visible light photocatalysis, *New Journal of Chemistry*, **2016**, *40*, 3000-3009.

18.Hazime, R.; Nguyen, Q. H.; Ferronato, C.; Salvador, A.; Jaber, F.; Chovelon, J. M. Comparative study of imazalil degradation in three systems: UV/TiO_2, UV/$K_2S_2O_8$ and UV/TiO_2/$K_2S_2O_8$, *Applied Catalysis B: Environmental*, **2014**, *144*, 286-291.

19.Deng, Y.; Ezyske, C. M. Sulfate radical-advanced oxidation process (SR-AOP) for simultaneous removal of refractory organic contaminants and ammonia in landfill leachate, *Water Res*, **2011**, *45*, 6189-6194.

20.Chen, W.-S.; Huang, C.-P. Mineralization of aniline in aqueous solution by electro-activated persulfate oxidation enhanced with ultrasound, *Chemical Engineering Journal*, **2015**, *266*, 279-288.

21.Chen, W. S.; Huang, C. P. Mineralization of aniline in aqueous solution by electrochemical activation of persulfate, *Chemosphere*, **2015**, *125*, 175-181.

22.Zhang, Z.; Wang, P. Optimization of photoelectrochemical water splitting

performance on hierarchical TiO_2 nanotube arrays, *Energy & Environmental Science*, **2012**, *5*, 6506-6512.

23.Wei, D. Formation and Crystallization Characteristics of Anodic Oxide Film on Pure Titanium in Potentiostatic Mode, *Journal of South China University of Technology*, **2012**, *40*, 30-36.

24.Mazzarolo, A.; Curioni, M.; Vicenzo, A.; Skeldon, P.; Thompson, G. E. Anodic growth of titanium oxide: Electrochemical behaviour and morphological evolution, *Electrochimica Acta*, **2012**, *75*, 288-295.

25.McManamon, C.; O'Connell, J.; Delaney, P.; Rasappa, S.; Holmes, J. D.; Morris, M. A. A facile route to synthesis of S-doped TiO_2 nanoparticles for photocatalytic activity, *Journal of Molecular Catalysis A: Chemical*, **2015**, *406*, 51-57.

26.Yang, G.; Wang, T.; Yang, B.; Yan, Z.; Ding, S.; Xiao, T. Enhanced visible-light activity of F-N co-doped TiO_2 nanocrystals via nonmetal impurity, Ti^{3+} ions and oxygen vacancies, *Applied Surface Science*, **2013**, *287*, 135-142.

27.Wu, J.-M.; Yin, J.-X. A facile solution-based approach to a photocatalytic active branched one-dimensional TiO_2 array, *RSC Advances*, **2015**, *5*, 3465-3469.

28.Sysoev, V. I.; Okotrub, A. V.; Gusel'nikov, A. V.; Smirnov, D. A.; Bulusheva, L. G. In situ XPS Observation of Selective NO_x Adsorption on the Oxygenated Graphene Films, *Phys Status Solidi B*, **2018**, *255*, 1700267.

29.Bendova, M.; Kolar, J.; Marik, M.; Lednicky, T.; Mozalev, A. Influence of nitrogen species on the porous-alumina-assisted growth of TiO_2 nanocolumn arrays, *Electrochimica Acta*, **2018**, *281*, 796-809.

30.Ananpattarachai, J.; Kajitvichyanukul, P.; Seraphin, S. Visible light absorption ability and photocatalytic oxidation activity of various interstitial N-doped TiO_2 prepared from different nitrogen dopants, *J Hazard Mater*, **2009**, *168*, 253-261.

31.Liu, Y.; Mu, K.; Zhong, J.; Chen, K.; Zhang, Y.; Yang, G.; Wang, L.; Deng, S.; Shen, F.; Zhang, X. Design of a solar-driven TiO_2 nanofilm on Ti foil by self-structure modifications, *RSC Advances*, **2015**, *5*, 41437-41444.

32.Fan, Y.; Ma, C.; Liu, B.; Chen, H.; Dong, L.; Yin, Y. Nitrogen doped anatase TiO_2 sheets with dominant {001} facets for enhancing visible-light photocatalytic activity, *Materials Science in Semiconductor Processing*, **2014**, *27*, 47-50.

33.Wang, W.; Lu, C.; Ni, Y.; Su, M.; Xu, Z. A new sight on hydrogenation of F and N-F doped {0 0 1} facets dominated anatase TiO_2 for efficient visible light photocatalyst, *Applied Catalysis B Environmental*, **2012**, *127*, 28-35.

34.Cheng, X.; Liu, H.; Chen, Q.; Li, J.; Wang, P. Construction of N, S codoped TiO_2 NCs decorated TiO_2 nano-tube array photoelectrode and its enhanced visible light photocatalytic mechanism, *Electrochimica Acta*, **2013**, *103*, 134-142.

35.Liu, D.; Zhou, J.; Wang, J.; Tian, R.; Li, X.; Nie, E.; Piao, X.; Sun, Z. Enhanced visible light photoelectrocatalytic degradation of organic contaminants by F and Sn co-doped TiO_2 photoelectrode, *Chemical Engineering Journal*, **2018**, *344*, 332-341.

36.Behpour, M.; Atouf, V. Study of the photocatalytic activity of nanocrystalline S, N-codoped TiO_2 thin films and powders under visible and sun light irradiation, *Applied Surface Science*, **2012**, *258*, 6595-6601.

37.Bhirud, A. P.; Sathaye, S. D.; Waichal, R. P.; Ambekar, J. D.; Park, C. J.; Kale, B. B.

In-situ preparation of N-TiO_2/graphene nanocomposite and its enhanced photocatalytic hydrogen production by H_2S splitting under solar light, *Nanoscale*, **2015**, *7*, 5023-5034.

38.Li, J.; Xu, X.; Liu, X.; Qin, W.; Pan, L. Novel cake-like N-doped anatase/rutile mixed phase TiO_2 derived from metal-organic frameworks for visible light photocatalysis, *Ceramics International*, **2017**, *43*, 835-840.

39.Zhou, F.; Song, H.; Wang, H.; Komarneni, S.; Yan, C. N-doped TiO_2/sepiolite nanocomposites with enhanced visible-light catalysis: Role of N precursors, *Applied Clay Science*, **2018**, *166*, 9-17.

40.Islam, M. M.; Basu, S. Understanding photoelectrochemical degradation of methyl orange using TiO_2 /Ti mesh as photocathode under visible light, *Journal of Environmental Chemical Engineering*, **2016**, *4*, 3554-3561.

41.Chen, C.; Ma, W.; Zhao, J. ChemInform Abstract: Semiconductor‐Mediated Photodegradation of Pollutants under Visible‐Light Irradiation, *Chemical Society Reviews*, **2010**, *39*, 4206-4219.

42.Zhang, Y.; Gu, D.; Zhu, L.; Wang, B. Highly ordered Fe^{3+} /TiO_2 nanotube arrays for efficient photocataltyic degradation of nitrobenzene, *Applied Surface Science*, **2017**, *420*, 896-904.

43.Ma, Q.; Wang, H.; Zhang, H.; Cheng, X.; Xie, M.; Cheng, Q. Fabrication of MnO_2/TiO_2 nano-tube arrays photoelectrode and its enhanced visible light photoelectrocatalytic performance and mechanism, *Separation and Purification Technology*, **2017**, *189*, 193-203.